

Optical correlator with variable discrimination capability — experimental results

MARÍA S. MILLÁN, ELISABET PÉREZ

Department of Optics and Optometry, Universitat Politècnica de Catalunya, C/Violinista Vellsolà 37, 08222 Terrassa, Barcelona, Spain.

RAFAŁ KOTYŃSKI, KATARZYNA CHALASIŃSKA-MACUKOW

Division of Information Optics, Institute of Geophysics, Faculty of Physics, Warsaw University, ul. Pasteura 7, 02-093 Warszawa, Poland.

In many pattern recognition applications it is required that the discrimination capability should be tunable. We propose and develop an optical set-up in which the discrimination capability could be continuously varied within a large range. Our set-up is based on the two-step JTC architecture. The pattern recognition algorithm that we realize using the set-up is the dual nonlinear correlation (DNC), which is a generalization of a number of popular filtering methods. The paper contains the results obtained numerically in a simulated optical set-up as well as the experimental results obtained in the optical correlator, which we built using two different SLMs. We analyse the correlator performance according to the different characteristics of the SLM panels.

1. Introduction

A considerable number of pattern recognition methods designed for the coherent optical correlators has been well-established in the last decades [1]. This becomes a motivation to introduce general models that would group the methods having a similar form. In the present paper we will deal with a model called the dual nonlinear correlation (DNC) [2]–[4].

The common study of filters unified within a model is not only elegant but also gives a better insight into the differences and similarities of their properties and enables one to compare the filtering methods in a systematic and reliable way. Moreover, since the model usually includes a number of methods, which have not been studied before, optimization of the method within the model results in obtaining new and in some terms better filters.

The first attempt to study a parametric family of correlation methods was made by KUMAR and HASSEBROOK [5], who established the model of the fractional power filters (FPF). The FPF generalize the classical matched filter, the phase only filter and the inverse filter. ERSOY and ZENG [6] considered a model of nonlinear filtering methods such that both the reference target and the input scene pass

through power-law nonlinearities before they are multiplied in the Fourier domain. A similar operation is achieved in the variant of the nonlinear joint transform correlator (JTC) of Javidi with the joint power spectrum being modified by a power-law nonlinearity [7].

The DNC that we introduced in [2] and [3] covers a wider class of filtering operations than the above mentioned models. The DNC encompasses nonlinear power-law processing operating independently on the spectra of the input image and the reference image. With the DNC model we built a connection between linear filtering methods and the nonlinear correlation methods intensively investigated in the last years.

We proposed to implement the DNC using the two-step JTC architecture [3]. Unlike the conventional linear JTC, our set-up is actually operated in three or four steps, since we need to capture not only the joint power spectrum but also the intensity of the input image spectrum and of the reference object spectrum. Afterwards, these spectra are subject to simple point processing which is done digitally. Finally, we display a modified joint power spectrum on the SLM. The DNC correlation is obtained in the output plane of the system, off the optical axis, similarly as in the conventional JTC.

The quality of optical pattern recognition is often characterized in terms of the standard performance criteria [5], such as the signal-to-noise-ratio (SNR), discrimination-capability (DC), or the peak-to-correlation-energy (PCE) ratio. In reference [3], we analyzed the dependence of DC and PCE on the most limiting characteristics of the SLM and CCD in a simulated optical set-up. In particular, we modelled the quantization and saturation introduced by the SLM and CCD. The results of this analysis were encouraging, as they indicated that the experimental realization of DNC is feasible with the use of commonly available SLMs, such as Epson VP-100PS.

In many applications, it is desired that there be the possibility of continuously varying the DC within a certain range of values. One may assume [4] that selective and variable DC could be obtained with use of the DNC. The recognition system may adapt its DC and become more sensitive to certain features of objects and more tolerant to other. In this sense, shape, intensity and colour variations were studied as features to which we were able to tune the discrimination of the DNC [4].

In this paper, we take advantage of all the aforementioned research on the DNC to build a real optoelectronic set-up that enables experimental implementation of the DNC. We present the experimental results obtained with the two-step JTC, which was intended for a recognition system with tunable discrimination to small distortions [3]. Our set-up uses an analog monochromatic CCD camera connected to an 8 bit frame-grabber and an electronically addressed SLM. In the experiments, we compare the results obtained with the use of two SLMs with different characteristics, namely Epson VP-100PS and CRL SVGA1. We discuss the influence of selected technical data of the SLM on the performance of the correlator.

2. Dual nonlinear correlator

2.1. Background

For the sake of simplicity we will use the one-dimensional notation. Let $s(x)$ and $r(x)$ denote the input signal, which is to be analyzed and the reference object that we seek. Their Fourier transforms will be denoted by capital symbols as $S(v)$ and $R(v)$, respectively. In a conventional linear correlator such as the JTC, the location of the target object $r(x)$ in the input scene $s(x)$ is estimated from the maximal values of intensity distribution of the correlation between $s(x)$ and $r(x)$, which can be obtained from their spectra according to expression

$$s(x) * r(x) = \text{IFT} \{S(v)R^*(v)\} \quad (1)$$

where $*$ denotes the correlation, and IFT – the inverse Fourier transform. The definition of the dual nonlinear correlation [2] extends Eq. (1) in a way that enables us to include in the same mathematical expression the filtering techniques that could not be realized by a linear correlator

$$\text{DNC}_{L,M}^{T(v)} \{s(x), r(x)\} = \text{IFT} \{T(v)|S(v)|^{L-1} |R(v)|^{M-1} S(v)R^*(v)\} \quad (2)$$

where L and M are some real coefficients and $T(v)$ is introduced as a real positive function, which could characterise the region of support in the Fourier plane (*e.g.*, the size of the aperture, or the scanning area of the CCD). In the following sections of the paper we assume that $T(v) \equiv 1$.

The DNC given in Eq. (2) could be seen as a parametric representation of a family of filtering methods, where any particular method is obtained for fixed values of L and M . The definition contains no singularities if $L, M > 1$, but in practice other values of L and M could also be used if any power of zero (also negative) is assumed to be equal to zero. If $L = 1$, the DNC defines a linear filtering operation (such as the classical matched filtering, phase-only or inverse filtering), otherwise the DNC is a nonlinear method (such as the pure phase correlation). Other well-known filtering operations, which are the particular cases of the DNC, are discussed in [2].

The choice of L and M has a direct influence on the system's discrimination capability [4] and other properties. For instance, the condition of $L = 0$ assures that the method is invariant to intensity of input image, while $L + M = 0$ is the condition that optimizes the peak-to-correlation-energy criterion [2].

Finally, we may note [2], [3] that independent of the choice of L and M , the DNC operation is shift-invariant, and assures that in the absence of noise the maximum of autocorrelation signal is located at the actual position of the target object. In this sense the DNC really generalizes the linear correlation-based pattern recognition methods.

2.2. Optical realization of the DNC

The optoelectronic implementation of the DNC could be based on a two-step JTC architecture (Fig. 1) [2], [3]. In the first step, three Fourier power spectra are

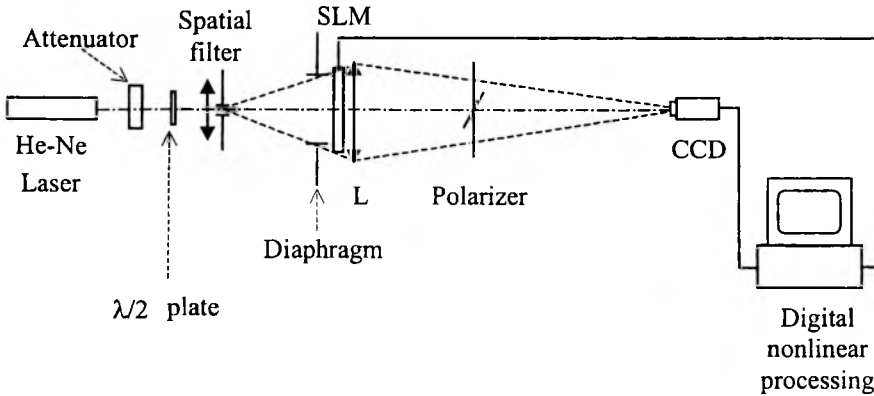


Fig. 1. Optoelectronic set-up based on JTC architecture that has been used in the experimental realization of the DNC.

sequentially captured by the CCD camera, which is placed in the focal plane of the set-up. The following spectra are captured: the reference power spectrum $I_R(v) = |R(v)|^2$, the input scene power spectrum $I_S(v) = |S(v)|^2$, and the joint power spectrum $I(v) = |\text{FT}\{r(x+d) + s(x-d)\}|^2$. The first two spectra are obtained by successively displaying the reference $r(x)$ and the input scene $s(x)$ on the electronically addressed spatial light modulator. The joint power spectrum $I(v)$ is captured in the classical way, after displaying both the reference and the input scene symmetrically shifted by the distance d from the center of the spatial light modulator.

Once the three power spectra $I(v)$, $I_S(v)$, and $I_R(v)$ are stored, the modified joint power spectrum $I'(v)$ is computed according to the following formula [3]:

$$I'(v) = I(v) I_S(v)^{(L-1)/2} I_R(v)^{(M-1)/2}. \tag{3}$$

Taking the inverse Fourier transform of the modified joint power spectrum $I'(v)$, we obtain the DNC between the input and the reference images. Then, it holds

$$\begin{aligned} \text{IFT}\{I'(v)\} = & O(x) + \text{DNC}_{L,M}\{s(x), r(x)\} \otimes \delta(x-2d) \\ & + \text{DNC}_{M,L}\{r(x), s(x)\} \otimes \delta(x+2d), \end{aligned} \tag{4}$$

where the symbol \otimes denotes the convolution and the irrelevant on-axis term $O(x)$ is equal to

$$O(x) = \text{IFT}\{|R(v)|^{M+1}|S(v)|^{L-1} + |R(v)|^{M-1}|S(v)|^{L+1}\}. \tag{5}$$

In the second step of JTC operation, the modified joint power spectrum $I'(v)$ is displayed on the spatial light modulator and its Fourier transform is obtained in the output plane. Since only direct (and not inverse) Fourier transforms can be obtained optically, the results obtained from a joint-transform correlator in the output plane differ from those expressed by Eq. (4) merely in an insignificant coordinate inversion ($x \rightarrow -x$). The on-axis term $O(x)$, (Eq. (4)), appears in the middle of the two off-axis DNC output signals. In the experiment, the overlapping between the on-axis and

off-axis terms can be avoided by introducing $[I(v) - I_S(v) - I_R(v)] + \text{const.}$ instead of $I(v)$ in the modified joint power spectrum $I'(v)$ of Eq. (3) so that the on-axis term $O(x)$ in Eq. (4) is reduced to $O(x) = \delta(x)$.

In this analysis we have assumed that the intensity distributions $I_R(v)$, $I_S(v)$, $I(v)$ and $I'(v)$ could be accurately captured by the CCD and displayed on the SLM. Unfortunately, the quantization introduced by these elements cannot be neglected. Moreover, the CCD may become saturated by the light of great intensity.

Our study of the influence of the experimental factors, such as the quantization or saturation, on the performance of the correlator [3] reveals that the CCD should be tuned to an operating range in which saturation actually occurs. As a result of saturation, the CCD cuts off the intense central peak of the captured power spectra, thus providing a more accurate representation of the high-frequency information.

2.3. Pattern recognition with continuously controlled DC

We use the following definition of the discrimination capability [4], [5]:

$$DC = \left| 1 - \frac{CC}{AC} \right| \leq u \tag{6}$$

where CC and AC denote the cross-correlation and autocorrelation intensities, respectively. The quotient (CC/AC) stands for the normalised cross-correlation and can be higher than unity dependent on the object energies and the non-linearities applied. We will denote by u the threshold applied to the correlation signal intensity, measured as a fraction of AC. In the following, we will arbitrarily set the threshold u to the value of 0.5. Thus, it can be deduced from Eq. (6) that the system is able to discriminate between two objects if their cross-correlation peak value differs by more than 50% of the autocorrelation peak value. Conversely, it may recognise two objects as the same if their cross-correlation peak value differs by no more than 50% of the autocorrelation peak value (*i.e.*, recognition is obtained if the condition $0.5 AC \leq CC \leq 1.5 AC$ is fulfilled).

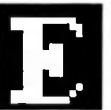
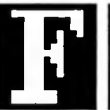
Reference object:	Input scenes:				
$r(x)$	$s_0(x) (=r(x))$	$s_1(x)$	$s_2(x)$	$s_3(x)$	$s_4(x)$
					
Normalized inner product: $cs_i = \frac{s_i(x)r(x)dx}{ r(x) ^2 dx}$					
	1	0.92	0.86	0.84	0.76

Fig. 2. Set of binary scenes used in the numerical and optical experiments.

Let us consider the set of test-images from Figure 2. The images are binary and have equal energies. The reference object is denoted as $r(x)$. The same figure also shows the normalized inner product of every image and the reference $r(x)$. The normalized inner product is commonly used to measure the similarity of two given images. Obviously, it depends on the application, whether objects which are actually very similar to the reference, such as those included in Fig. 2, should be classified as distorted reference objects, or as false targets. We may wish to relate this decision to the value of the inner product. However, in a real application, it would be more convenient to have the possibility of tuning the discrimination capability.

We simulated numerically the optical set-up described in the preceding subsection. We assumed that the CCD and SLM uniformly quantize the signal, into 256 and 32 intensity levels, respectively. In addition, the camera becomes saturated in the first step of JTC, when the dynamics of the captured intensity distributions are larger than in the second step. We model the saturation effect as a thresholding, which occurs at 10% of the maximal value of the joint power spectrum.

We varied the parameters L and M in the range from -1 to $+1.4$ with the step of 0.2 and calculated the corresponding DNC for every image from Fig. 2, with $r(x)$ as the reference object. Then, for each of the test-objects we subdivided the $L - M$ space into the region where the object was successfully discriminated from the

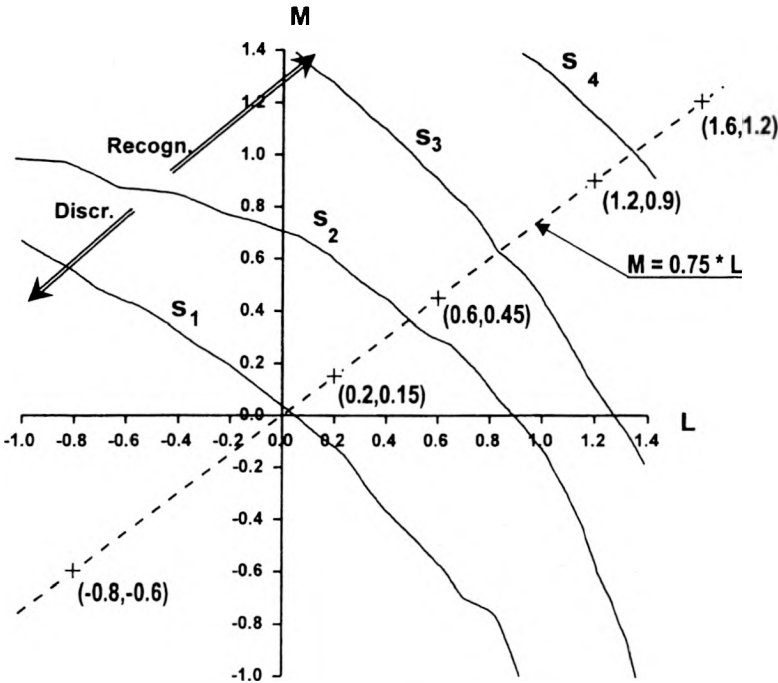


Fig. 3. Boundary-lines that separate the region of the $L - M$ space, in which the corresponding object is recognized as the reference (Recogn.), and the complementary region in which the same object is successfully discriminated from the reference (Discr.). The axis $M = 0.75 L$ has the values of (L, M) used for the experiment marked on it.

reference, and the complementary region where the object was recognized as equal to the reference.

Figure 3 presents the plot of the boundary-lines that divide the $L - M$ space into those subregions.

The boundary-lines appear ordered in such a way that the closer the line is to the coordinate origin, the higher the value of the corresponding inner product of the object with the reference (Fig. 2). The position of a boundary-line with regard to the others accounts for this measurement of similarity between the corresponding test-object and the reference.

In the upper right quadrant of the $L - M$ plane, for low values of L and M , the system has high discrimination capability, whereas for high values of L and M , the system has low discrimination capability. In fact, the smaller the values of L and M , the higher spatial frequencies are emphasized causing the system to become more sensitive to distortions. Conversely, the higher the values of L and M , the lower frequencies are emphasized. Usually, small distortions do not affect the low-frequency content of the original image. Thus, the choice of high values of L and M makes the recognition system more tolerant to distortions.

According to the simulations presented in Figure 3, if we were able to tune the values of L and M , for example, along the axis $L = M$ or an axis close to this (e.g., axis $M = 0.75 L$ is shown in Fig. 3), we could vary the discrimination capability in a continuous way within a large range of values. In fact, the optical implementation of the DNC, which we will present in the following section, enables us to tune the DC in an almost continuous way.

3. Discussion of the optically obtained results

The dual nonlinear correlator was built on a JTC basis (Fig. 1). A b/w CCD camera (Pulnix TM-765) of 8-bits (256 grey levels) with a saturation level of 10% was used to register power spectra in the first step of the DNC. As SLM we separately

Table 1. Technical characteristics of Epson and CRL spatial light modulators.

Characteristic	Epson	CRL
Model	VP-100PS	SVGA1
Panel size	25 (H) × 10 (V) mm	26.4 (H) × 19.8 (V) mm
Resolution	320 (H) × 264 (V) pixels	800 (H) × 600 (V) pixels
Actual resolution*	224 (H) × 256 (V) pixels	800 (H) × 600 (V) pixels
Pixel size	55 (H) × 50 (V) μm	26 (H) × 24 (V) μm
Pixel pitch	83.1 (H) × 74.8 (V) μm	33 (H) × 33 (V) μm
Active area	44%	57%
Transmission	43%	11%
Contrast ratio	80:1	200:1
Modulation	Continuous grayscale	Continuous grayscale
Operating control	Raw by raw	Pixel by pixel

*There are some pixels not accessible with the electronics.

used two devices, an Epson SLM and a CRL SLM, whose technical characteristics are specified in Tab. 1. Data about transmission efficiency (for $\lambda = 0.6328 \mu\text{m}$) and contrast of Epson panels were taken from [8].

Clearly, CRL SLM has better resolution and contrast but worse transmission efficiency than Epson SLM. Graphs of the transmitted intensity (in arbitrary units) versus the grey level codified to be displayed on the SLM are shown in Figs. 4a and b for Epson and CRL devices, respectively. The slope in the Epson SLM graph is less steep than in the CRL graph. This is related to the number of grey levels that can be actually addressed by each SLM. Thus, whereas we could linearly address about 20 by Epson SLM, we could only linearly address about 10 grey levels by CRL SLM. These numbers of grey levels were lower if only the linear part of the graphs was considered in both SLM. Then, Epson SLM could display about 10 grey levels and CRL SLM could display about 6.

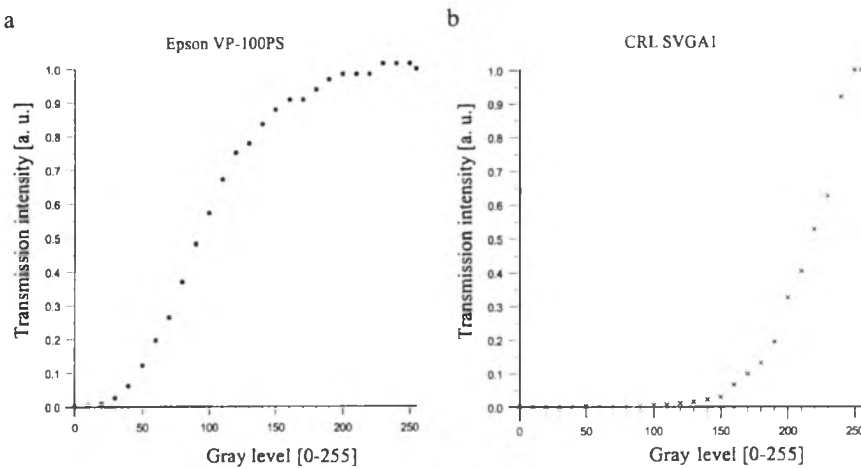


Fig. 4. Transmission characteristics of the: **a** – Epson SLM, **b** – CRL SLM. The intensity transmission in arbitrary units is plotted versus the level of the 8-bit driving digital video signal.

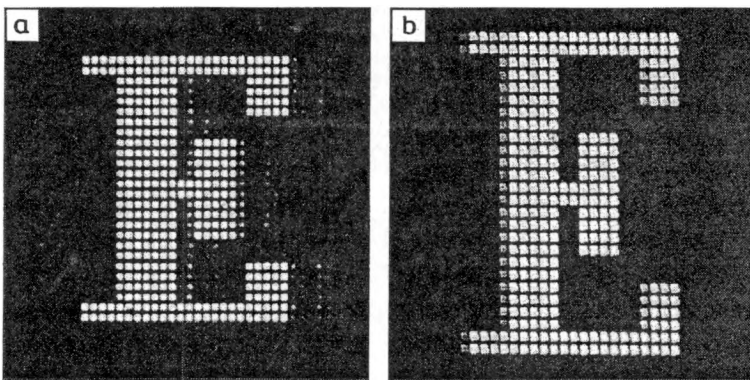


Fig. 5. Binary letters reproduced by: **a** – Epson VP-100PS, and **b** – CRL SVGA1 panels.

This fact has no relevance in the first step of the DNC, when the SLM is only used to display the input binary signals. For instance, in Fig. 5 binary segmented letters are reproduced as they were displayed by the SLMs. In this example, the signal (reference letter of the test) is better reproduced by CRL SLM than by Epson SLM, because the Epson SLM activates some extra columns of the panel in the edges of the letter and also in the middle of the background. But this is not the same case in the second step of the DNC, when the nonlinearly modified joint power spectrum is displayed on the SLM. In this case, a wide dynamic range of grey levels is preferable to obtain a recognition system able to reproduce the different nonlinearities introduced by the values of parameters L and M of DNC. This need is particularly important for high positive values of L and M . Figures 6 and 7 show an example of this case. Figure 6 corresponds to the logarithm of the modified joint-power spectrum intensity of the letter $s_2(x)$ (scene) and $r(x)$ (reference) calculated by numerical simulation with $L = 1.2$, $M = 0.9$ and assuming a saturation level of 10% and 256 grey levels for acquisition by camera. Figures 7a, b show the logarithms of this intensity distribution as is experimentally displayed by Epson SLM and CRL SLM, respectively. From these figures, it can be noted that the intensity distribution displayed by CRL SLM is poorer in grey levels than that displayed by Epson SLM.

Table 2 presents the experimental results of the normalised correlation intensity obtained using Epson SLM in the dual non-linear correlator. Objects whose experimental normalised cross-correlation intensity fulfils $0.5 \leq CC/AC \leq 1.5$ are recognised as the reference object; otherwise, they are discriminated. Table 3 presents experimental results obtained using CRL SLM instead. Considering the points marked along the axis $M = 0.75L$ in Fig. 3, L and M values were selected in the

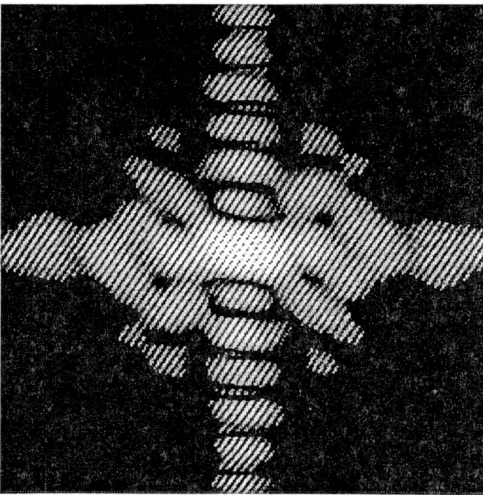


Fig. 6. Logarithm of the modified joint power spectrum $I'(v)$. The image was obtained in the numerical simulation of the optical set-up, where we assumed that $r(x)$ is the reference, $s_2(x)$ is the input image, $L = 1.2$, $M = 0.9$, and the CCD saturation level is equal to 10%.

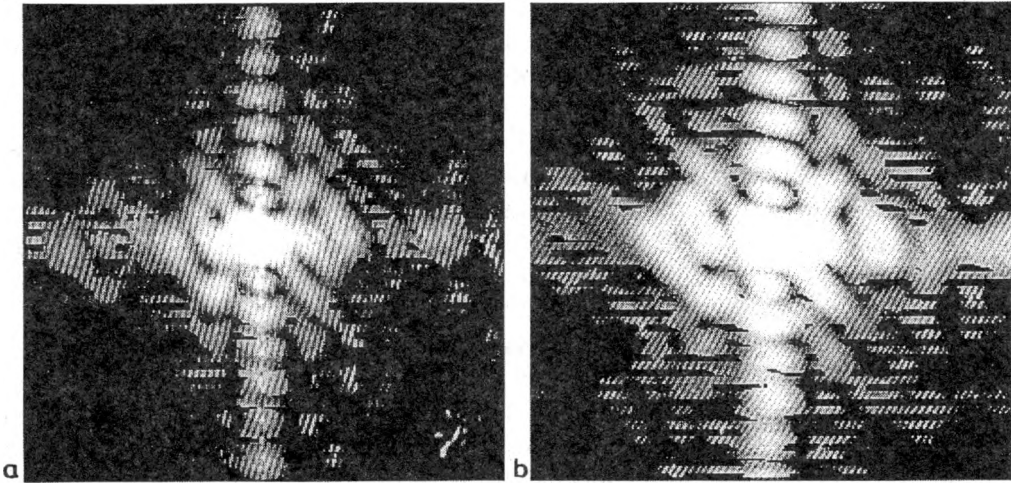


Fig. 7. The same modified power as in Fig. 6, however, here the results were obtained by the SLMs. The power spectrum is displayed on the Epson panel (a) and the CRL panel (b).

Table 2. Normalized correlation signal intensities obtained in the optical DNC correlator. The set-up includes the SLM from Epson. Figures in brackets come from numerical simulations, and are given for comparison with the experimental results. When the experimental normalised correlation intensity $0.5 \leq CC/AC \leq 1.5$, the input object is recognised as the reference. This situation is indicated by "Yes" in the "Recogn." fields of the table.

Input image	$r(x)$	$s_1(x)$	$s_2(x)$	$s_3(x)$	$s_4(x)$
$(L = -0.8, M = -0.6)$	1 (1)	0.47 (0.24)	0.41 (0.17)	0.23 (0.04)	0.27 (0.05)
Recogn.	Yes	No	No	No	No
$(L = 0.2, M = 0.15)$	1 (1)	0.67 (0.57)	0.49 (0.41)	0.34 (0.21)	0.30 (0.19)
Recogn.	Yes	Yes	No	No	No
$(L = 0.6, M = 0.45)$	1 (1)	0.79 (0.68)	0.56 (0.52)	0.41 (0.38)	0.39 (0.27)
Recogn.	Yes	Yes	Yes	No	No
$(L = 1.2, M = 0.9)$	1 (1)	0.82 (0.76)	0.62 (0.68)	0.54 (0.75)	0.45 (0.48)
Recogn.	Yes	Yes	Yes	Yes	No
$(L = 1.6, M = 1.2)$	1 (1)	0.75 (0.76)	0.65 (0.71)	0.61 (0.91)	0.46 (0.63)
Recogn.	Yes	Yes	Yes	Yes	No

experiment to obtain a wide range of discrimination capability of the recognition system. For example, for $(L, M) = (-0.8, -0.6)$ a highly discriminative system was intended. Conversely, for $(L, M) = (1.6, 1.2)$ a tolerant system was intended. The experimental results are presented along with the simulated results (in brackets). The simulated results were digitally obtained under the experimental conditions described in Sect. 2 for the acquisition system (a camera working with 10% of saturation level and 256 grey levels) and taking into account a dynamic range of 20 grey levels for the Epson SLM (Tab. 2) and 10 grey levels for CRL SLM (Tab. 3).

Table 3. Same information as in Tab. 2, but for the set-up with the CRL SLM.

Input scene	$r(x)$	$s_1(x)$	$s_2(x)$	$s_3(x)$	$s_4(x)$
$(L = -0.8, M = -0.6)$	1 (1)	0.43 (0.22)	0.30 (0.15)	0.27 (0.03)	0.32 (0.05)
Recogn.	Yes	No	No	No	No
$(L = 0.2, M = 0.15)$	1 (1)	0.62 (0.57)	0.62 (0.41)	0.35 (0.22)	0.36 (0.20)
Recogn.	Yes	Yes	No	No	No
$(L = 0.6, M = 0.45)$	1 (1)	0.72 (0.76)	0.80 (0.60)	0.40 (0.47)	0.43 (0.33)
Recogn.	Yes	Yes	Yes	No	No
$(L = 1.2, M = 0.9)$	1 (1)	0.73 (0.71)	0.80 (0.70)	0.51 (0.79)	0.57 (0.52)
Recogn.	Yes	Yes	Yes	Yes	Yes
$(L = 1.6, M = 1.2)$	1 (1)	0.71 (0.78)	0.84 (0.70)	0.48 (1.01)	0.61 (0.72)
Recogn.	Yes	Yes	Yes	No	Yes

Basically, both modulators allowed us to obtain a recognition system with variable discrimination capability depending on the L, M values in the DNC. In some cases, for which the numerical result is near the threshold, the eventual recognition result differs from the predicted one, but we think there are only few such cases and these are not representative of the general performance of the system. Comparing the performances of Epson and CRL SLMs there is not a clear advantage in using one of them instead of the other. When reducing the number of grey levels that can be addressed by the SLM, in our case it means using CRL SLM, a slightly higher tolerance to shape changes can be appreciated, particularly for $(L, M) > (0.6, 0.45)$. Then, for our recognition purposes, this result leads us to appreciate in modern SLMs not only their resolution, but also their grey level dynamic range.

4. Conclusions

We have simulated, built and tested an optical correlator for pattern recognition. The set-up is based on the 2-step JTC architecture, and is capable of realizing recognition algorithms that can be expressed with the DNC model.

We tested the correlator performance from the point of view of its discrimination capability. We obtained a system in which it was possible to vary the tolerance to small distortions of the object shape. By selecting the values of real parameters L and M , we controlled the severity of nonlinearities applied in the spectral domain and therefore the discrimination capability of the system could be tuned from certain tolerance to high discrimination. The numerical and optical results confirm that the high and positive value of L and M leads to increased tolerance to distortions whereas low or negative values of L and M lead to a higher discrimination capability.

We tested the set-up with two different liquid crystal twisted-nematic SLMs – one from Epson and the other from CRL. The CRL SLM provides better

resolution, higher contrast, and lower cross-talk between pixels, but its intensity transmittance is strongly nonlinear. In fact, we did not observe any significant improvement in the set-up performance when we replaced the old Epson SLM by the modern CRL SLM.

Basically, we obtained encouraging results with both SLMs, and we were able to vary the discrimination capability in a similar range of values, in both cases.

References

- [1] CAMPOS J., TURON F., YAROSLAVSKY L.P., YZUEL M.J., *Int. J. Opt. Comp.* **2** (1991), 341.
- [2] KOTYŃSKI R., CHAŁASIŃSKA-MACUKOW K., *J. Mod. Opt.* **43** (1996), 295.
- [3] PEREZ E., CHAŁASIŃSKA-MACUKOW K., STYCZYŃKI K., KOTYŃSKI R., MILLAN M.S., *J. Mod. Opt.* **44** (1997), 1535.
- [4] MILLAN M.S., PEREZ E., CHAŁASIŃSKA-MACUKOW K., *Opt. Commun.* **161** (1999), 115.
- [5] KUMAR V., HASSEBROOK L., *Appl. Opt.* **29** (1990), 2997.
- [6] ERSOY K., ZENG M., *J. Opt. Soc. Am. A* **6** (1989), 636.
- [7] JAVIDI B., *Patt. Recogn.* **27** (1994), 523.
- [8] KIRSCH J.C., GREGORY D.A., THIE M.W., JONES B.K., *Opt. Eng.* **31** (1992), 963.

Received May 22, 2000